Dirac soliton stability and interaction in binary waveguide arrays

Truong X. Tran,[1,2,*] Xuan N. Nguyen,[1] and Dũng C. Duong[1]

[1]*Department of Physics, Le Quy Don University, 236 Hoang Quoc Viet str., 10000 Hanoi, Vietnam*
[2]*Max Planck Institute for the Science of Light, Günther-Scharowsky str. 1, 91058 Erlangen, Germany*
**Corresponding author: truong.tran@mpl.mpg.de*

Received February 6, 2014; revised March 22, 2014; accepted March 25, 2014;
posted March 25, 2014 (Doc. ID 206068); published April 22, 2014

We analyze the stability of a recently found exact analytical spatial soliton in binary waveguide arrays—an analog of the relativistic Dirac soliton. We demonstrate that this soliton class is very robust. The soliton dynamics and different scenarios of soliton interactions are systematically investigated. © 2014 Optical Society of America

OCIS codes: (190.6135) Spatial solitons; (190.4370) Nonlinear optics, fibers; (230.7370) Waveguides.
http://dx.doi.org/10.1364/JOSAB.31.001132

1. INTRODUCTION

Waveguide arrays have been used intensively to simulate the evolution of a nonrelativistic quantum mechanical particle in a periodic potential [1]. Many fundamental phenomena in nonrelativistic classical and quantum mechanics, such as Bloch oscillations [2,3], Zener tunneling [4,5], optical dynamical localization [6], and Anderson localization in disordered lattices [7], have been investigated both theoretically and experimentally by using waveguide arrays. In recent studies it was shown that, rather surprisingly, most of the nonlinear phenomena usually associated with fiber optics (such as the emission of resonant radiation from solitons and soliton self-wavenumber shift) can also take place in specially excited waveguide arrays, but in the spatial domain rather than in the temporal domain [8,9]; and the supercontinuum in both frequency and wavenumber domains can be generated in nonlinear waveguide arrays [10]. Binary waveguide arrays (BWAs) have also been used to mimic relativistic phenomena typical of quantum field theory, such as Klein tunneling [11,12], *Zitterbewegung* (trembling motion of a free Dirac electron) [13,14], and fermion pair production [15], which are all based on the properties of the Dirac equation [16]. Quite recently, the optical analog of relativistic Dirac solitons has been analytically found in BWAs [17]. In [17], we have provided analytical expressions for the nonmoving gap solitons in BWAs. We have also shown their connection to Dirac solitons in a nonlinear extension of the relativistic one-dimensional (1D) Dirac equation describing the dynamics of a freely moving relativistic particle. Similar soliton solutions have been found for the nonlinear 1D Dirac equation [18], but with a different and more complicated kind of nonlinearity, in the context of quantum field theory. The discrete gap solitons in BWAs in the *classical* context have been investigated both numerically [19–21] and experimentally [22]. Although there is currently no evidence for fundamental quantum nonlinearities, nonlinear versions of the Dirac equation have been studied for a long time. One of the earlier extensions was investigated by Heisenberg [23] in the context of field theory and was motivated by the question of mass. In the quantum mechanical context, nonlinear Dirac equations have been used as effective theories in atomic, nuclear, and gravitational physics [24–27] and, more recently, in the study of ultracold atoms [28,29]. To this regard, BWAs can offer a unique platform to simulate nonlinear extensions of the Dirac equation when probed at high light intensities. One of these possibilities is to use BWAs as a classical simulator of the Dirac equation to mimic the two-body Dirac model, i.e., the Dirac equation for two interacting relativistic particles, which has attracted interest of researchers since the early days of quantum mechanics [30,31].

Motivated by our recent achievements in the investigation of the optical analog of the relativistic Dirac solitons in BWAs, by the importance of BWAs as a classical simulator for relativistic quantum phenomena, in this work we study the stability of the newly found exact analytical spatial solitons in BWAs (for brevity, further referred to as Dirac solitons). We then investigate the features of the interaction between Dirac solitons, and also show how to generate the transversely moving Dirac solitons from motionless Dirac solitons in BWAs. This paves the way for using BWAs to simulate nonlinear extensions of the Dirac equation, as well as other solitonic and nonsolitonic effects of nonlinear Dirac equations.

2. DIRAC SOLITON STABILITY

Light propagation in a discrete, periodic binary array of Kerr nonlinear waveguides can be described, in the continuous-wave regime, by the following dimensionless coupled-mode equations (CMEs) [19]:

$$i\frac{da_n(z)}{dz} = -\kappa[a_{n+1}(z) + a_{n-1}(z)] + (-1)^n\sigma a_n - \gamma|a_n(z)|^2 a_n(z), \tag{1}$$

where a_n is the electric field amplitude in the nth waveguide, z is the longitudinal spatial coordinate, 2σ and κ are the propagation mismatch and the coupling coefficient between two adjacent waveguides of the array, respectively, and γ is the nonlinear coefficient of the waveguides. As mentioned above,

the analytical Dirac soliton solutions to the CMEs for BWAs have been found as follows [17]:

$$\begin{bmatrix} a_{2n}(z) \\ a_{2n-1}(z) \end{bmatrix} = \begin{bmatrix} i^{2n}\frac{2\kappa}{n_0\sqrt{\sigma\gamma}}\mathrm{sech}\left(\frac{2n}{n_0}\right)e^{iz\left(\frac{2\kappa^2}{n_0^2\sigma}-\sigma\right)} \\ i^{2n}\frac{2\kappa^2}{n_0^2\sigma\sqrt{\sigma\gamma}}\mathrm{sech}\left(\frac{2n-1}{n_0}\right)\tanh\left(\frac{2n-1}{n_0}\right)e^{iz\left(\frac{2\kappa^2}{n_0^2\sigma}-\sigma\right)} \end{bmatrix}. \quad (2)$$

This analytical Dirac soliton solution in BWAs is a one-parameter family where one parameter, such as soliton peak amplitude or width, can be arbitrary, provided that the soliton width is large enough (the beam width parameter $n_0 \geq 3.5$, see [17] for more details). The Dirac soliton solution in the form of Eq. (2) is valid in the case when γ and σ are positive. However, with this solution one can easily construct other Dirac soliton solutions for any sign of each parameter γ and σ [17]. First of all, let us assume that $(a_{2n}, a_{2n-1})^T = i^{2n}(\varphi_{2n}, \varphi_{2n-1})^T$ is one solution of Eq. (1). In this case, if we change the sign of γ while keeping the other parameters constant, one can easily show that a new solution of Eq. (1) will be $(a_{2n}, a_{2n-1})^T = i^{2n}(\varphi^*_{2n-1}, \varphi^*_{2n})^T$, where $*$ denotes the complex conjugation. Second, if the sign of σ is changed while the other parameters are kept constant, then a new solution of Eq. (1) will be $(a_{2n}, a_{2n-1})^T = i^{2n}(\varphi_{2n-1}, \varphi_{2n})^T$.

The fact that one can analytically find Dirac solitons in BWAs gives a hint that Dirac solitons found in this system should be stable as the fundamental soliton obtained from the well-known nonlinear Schrödinger equation (NLSE) describing temporal solitons in a single optical fiber [32], or spatial solitons in a single waveguide [33], which can also be analytically obtained by the inverse scattering transform method [34]. In order to investigate the soliton stability two different approaches are often adopted. The first approach is based on the linear stability analysis [32] where a weak noise signal is superimposed with the exact soliton solution, then linearized equations are obtained for the low-amplitude modes, and finally their gain spectrum is calculated. This linear stability analysis, which requires both analytical and numerical work, could give valuable physical insights and can be easily implemented, provided that the number of governing equations is limited. In the case of BWAs where a large number of waveguides is used, the above approach could be quite cumbersome. In the second approach, the input pulse (or beam) which does not correspond to the exact soliton solutions is used to numerically simulate the propagation of the pulse (or beam) in the system. Based on the propagation features, conclusions can be drawn regarding the soliton stability. In this work, we use the latter approach to check the Dirac soliton stability.

Supposing that ψ_n is the exact analytical Dirac soliton solution to Eq. (1) [17], we investigate the propagation of the initial beam (quasi-soliton) $a_n = r\psi_n$, where $r \simeq 1$. Figures 1(a) and 1(b) show the propagation of two beams with $r = 1.15$ and 0.85, respectively, where Eq. (1) is integrated with these initial conditions. The input and output beam profiles in Figs. 1(a) and 1(b) are shown, respectively, in Figs. 1(c) and 1(d). From Figs. 1(a) and 1(b) one can see that although the input beams are not the exact Dirac solitons, these quasi-solitons still propagate robustly inside BWAs without any significant change of the initial beam shapes. Of course, because the input beams are not the exact Dirac solitons, they cannot perfectly maintain the shapes during propagation as compared to the exact solitons, and one can see radiations emitted from the beams during propagation in Figs. 1(a) and 1(b). By analyzing Figs. 1(c) and 1(d) one can conclude that the beam profiles will evolve toward those of the exact Dirac solitons during propagation. Indeed, Figs. 1(c) and 1(d) show two components of the input beams (the red solid curve plots the strong component $|a_{2n}|$ at even waveguide positions, whereas the red dashed curve plots the weak component $|a_{2n-1}|$ at odd waveguide positions), two components of the output beams (the black solid curve plots the strong component $|a_{2n}|$ at even waveguide positions, whereas the black dashed curve plots the weak component $|a_{2n-1}|$ at odd waveguide positions), and also the exact analytical soliton profiles with discrete blue circles. Here we take the peak amplitude of the output beams [$|a_0| = 0.475$ and 0.266 for Figs. 1(c) and 1(d), respectively] to analytically find the exact Dirac solitons. One can clearly see that the output beam profiles and the profiles of the exact Dirac solitons shown in Figs. 1(c) and 1(d) are in good agreement with each other. The simulations with other values for parameter $r \simeq 1$ (not shown here) help us conclude that Dirac solitons are indeed stable with respect to perturbations. When the parameter $r > 1$, the quasi-soliton will evolve toward the Dirac soliton with higher peak amplitude, and thus narrower beam width [see Fig. 1(c)]. Meanwhile, with the parameter $r < 1$, the quasi-soliton will evolve toward the Dirac soliton with lower peak amplitude, and thus wider beam width [see Fig. 1(d)]. Our simulations reveal that for parameters used in Fig. 1 the value of r can even get the lower limit $r = 0.65$ for which Dirac solitons still can be established during propagation. If $r < 0.65$, then the beam will keep on broadening during propagation, and thus Dirac solitons cannot be formed. If $r > 1.5$, it is possible to form high-order Dirac solitons, but this topic will be covered elsewhere in a future publication. To estimate real physical parameters of the calculated solitons we use typical parameters in waveguide arrays made of AlGaAs [3], where the coupling coefficient and nonlinear coefficient in physical units are $K = 1240\ \mathrm{m}^{-1}$ and $\Gamma = 6.5\ \mathrm{m}^{-1}\ \mathrm{W}^{-1}$, respectively. In this case, the power scale will be $P_0 = K/\Gamma = 190.8$ W, thus the peak power of the soliton shown in Figs. 1(c) and 1(d) will

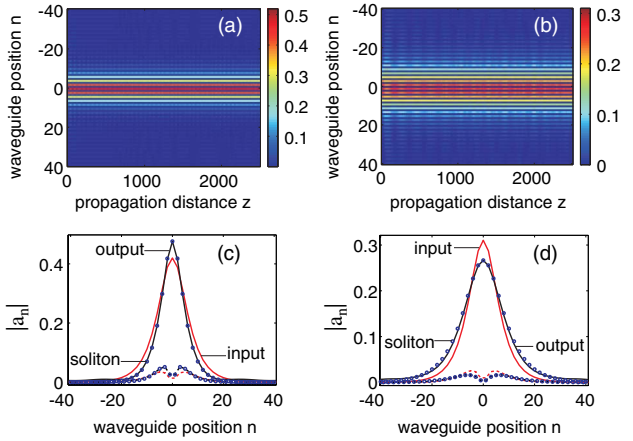

Fig. 1. Formation of the Dirac solitons during the propagation of beams, which are initially different from the exact Dirac solitons. (a), (b) Propagation of beams with parameter $r = 1.15$ and 0.85, respectively. (c), (d) The input and output beam profiles with parameter $r = 1.15$ and 0.85, respectively. Parameters: $\kappa = 1$; $\gamma = 1$; $\sigma = -1.2$; and beam width parameter $n_0 = 5$.

be around 43.0 and 13.5 W, respectively, and the length scale in the propagation direction will be $z_0 = 1/K = 0.8$ mm.

3. DIRAC SOLITON INTERACTION

It is clear on physical backgrounds that two and more solitons would begin to affect each other only when they are close enough that their tails overlap. In this section, we investigate the interaction of Dirac solitons where two and more Dirac solitons are brought together close enough. Figure 2 shows different scenarios of the interaction of two Dirac solitons when using the input condition $a_n(0) = \psi_{n+\Delta n}(0) + r\psi_{n-\Delta n}(0)\exp(i\theta)$ (with $2\Delta n$ being the initial center-to-center spacing and θ being the initial phase difference between two solitons) for numerically solving Eq. (1). Figures 2(a)–2(c) demonstrate the interaction of two Dirac solitons that are initially identical ($r = 1$) with initial phase difference $\theta = 0, \pi/2$, and π, respectively. It is well known that two identical NLSE solitons attract each other in the in-phase case ($\theta = 0$), exchange energy then repel each other in the case $\theta = \pi/2$, and repel each other even more strongly in the out-of-phase case ($\theta = \pi$) [32,33]. These features of the interaction between two identical NLSE solitons can also be seen in the interaction of two Dirac solitons where two identical Dirac solitons attract each other in the in-phase case ($\theta = 0$) [see Fig. 2(a)], exchange energy then repel each other in the case $\theta = \pi/2$ [see Fig. 2(b)], and repel each other even more strongly in the out-of-phase case ($\theta = \pi$) [see Fig. 2(c)]. The main difference between the interaction of two identical NLSE solitons and that of two identical Dirac solitons is in the in-phase case. For the case of NLSE solitons, two in-phase NLSE solitons after being launched into the system will attract each other, then merge into one single structure for the first time at the propagation distance z_0, then separate from each other, and then collide periodically along the fiber with the period $\Delta z = 2z_0$ (see Fig. 5.18 in [32]). Whereas in the case of Dirac solitons, as seen from Fig. 2(a), two in-phase Dirac solitons attract each other, then merge at the distance $z_0 = 476$, but after that two beams *aperiodically* separate from each other and collide with each other at much shorter distance as compared to the stable period $\Delta z = 2z_0$ for NLSE solitons, and finally form a single beam. It is obvious that if the initial center-to-center spacing between two solitons is reduced (increased), then the interaction between them will be enhanced (less strong). It is well known than if one NLSE soliton interacts with another in-phase NLSE quasi-soliton (for instance, when $r = 1.1$, see Fig. 5.18 in [32]), then they will oscillate periodically, but never collide or keep moving far away from each other. This feature also repeats exactly with Dirac solitons as demonstrated in Fig. 2(d) with $r = 1.1$. Here the periodic oscillation of solitons is not clearly seen, but if the parameter r gets smaller, then the oscillation will be enhanced (not shown here).

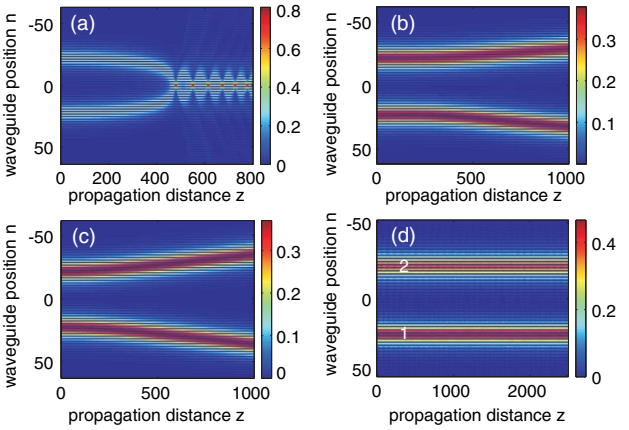

Fig. 2. Interaction of two Dirac solitons. (a)–(c) Interaction of two Dirac solitons that are initially identical with initial phase difference $\theta = 0, \pi/2$, and π, respectively. (d) Interaction of one Dirac soliton with another in-phase Dirac quasi-soliton with $r = 1.1$. Parameters: $\Delta n = 22$; the other ones are the same as in Fig. 1.

Figure 3 illustrates the interaction of three Dirac solitons. Figure 3(a) shows the interaction of three identical in-phase Dirac solitons that are equally spaced at the input. At the beginning they attract each other and two solitons on wings move toward the central soliton (as expected), but unlike the case of two identical in-phase Dirac solitons, three Dirac solitons in Fig. 3(a) will not collide. At the later stage, two solitons on wings will separate from the central one and keep moving far away from each other. The latter feature is not present in the case of NLSE solitons. Our simulations (not included here) show that three identical in-phase NLSE solitons will attract each other, then separate from each other, then attract each other again, and the cycle repeats so on, but they never keep moving far away from each other. As in the case for two in-phase Dirac quasi-solitons [see Fig. 2(d)], it is possible to form a complex consisting of three in-phase Dirac quasi-solitons where each Dirac quasi-soliton can oscillate, but they never collide or keep moving far away from each other [see Figs. 3(b) and 3(c)]. In Fig. 3(b) the initial peak amplitude of quasi-solitons decreases monotonically from the first to third quasi-solitons: $r_1 = 1.05$; $r_2 = 1.0$; $r_3 = 0.95$, where the ith quasi-soliton is formed by multiplying the exact soliton solution with the factor r_i, and i is the soliton label indicated in Figs. 3(b) and 3(c). In Fig. 3(c) the peak amplitude of the central soliton is initially smaller than that of the other

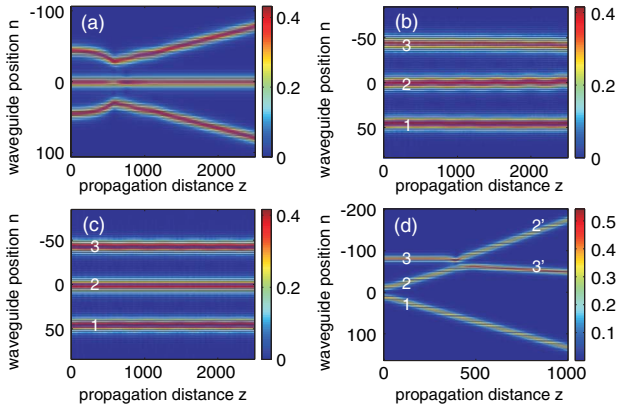

Fig. 3. Interaction of three Dirac solitons. (a) Solitons are initially identical. (b) Initial peak amplitude decreases monotonically from the first to third quasi-solitons: $r_1 = 1.05$; $r_2 = 1.0$; $r_3 = 0.95$. (c) Peak amplitude of the central soliton is initially smaller than that of two quasi-solitons on wings: $r_1 = 1.05$; $r_2 = 1.0$; $r_3 = 1.05$. Solitons are in-phase in (a)–(c). (d) The first two solitons have the same amplitude at the beginning with beam width parameter $n_0 = 5$, but the width of the third soliton is reduced by a factor of 0.9 as compared to that of the first two solitons. The second and third solitons are in-phase, but out-of-phase with the first soliton. Solitons on wings are initially equidistant from the central soliton in (a)–(c), but have different initial center-to-center distances in (d). Parameters: $\kappa = 1$; $\gamma = 1$; $\sigma = -1.2$; beam width parameter $n_0 = 5$ for quasi-solitons in (a)–(c).

two quasi-solitons on wings: $r_1 = 1.05$; $r_2 = 1.0$; $r_3 = 1.05$. The initial center-to-center spacing between two adjacent Dirac solitons (or quasi-solitons) in Figs. 3(a)–3(c) is 44 waveguides.

The single exact analytical Dirac soliton found in [17] is transversely motionless in the sense that it does not move in the transverse direction across BWAs, and its direction is just parallel to that of each waveguide. Thus, so far in this paper, initially, all Dirac solitons launched at the input of BWAs are also transversely motionless. In principle, the Dirac solitons that move transversely (for brevity, further referred to as moving Dirac solitons) can be numerically found by applying, for instance, the shooting method [35] to Eq. (1). But with a large number of waveguides the shooting method will be rather cumbersome. Another method to obtain the moving Dirac solitons is simple and straightforward just through the interaction of two out-of-phase motionless Dirac solitons as shown in Fig. 2(c). The transverse speed of moving Dirac solitons can be easily controlled by varying the initial distance between two out-of-phase motionless Dirac solitons. In Fig. 3(d) we show the interaction of the motionless Dirac soliton (third soliton) with a moving Dirac soliton (second soliton). At the input three Dirac solitons are all motionless. The second and third solitons are initially in-phase, but out-of-phase with the first soliton. The initial center of the first, second, and third solitons is located at the waveguide with position $n = 12, -12, -80$, respectively. The first two solitons have the same peak amplitude at the beginning with beam width parameter $n_0 = 5$, but the width of the third soliton is reduced by the factor of 0.9 as compared to the width of the first two solitons, thus its peak amplitude is increased by a factor of $1/0.9$ as compared to that of the first two solitons. At the beginning, due to the great distance between the third soliton and the other two solitons, the third soliton practically does not interact with the other two solitons, thus it just propagates along the z axis. Meanwhile, the distance between two out-of-phase first and second solitons is short, thus they repel each other and the second soliton moves up toward the third one. At the distance $z \simeq 390$, the center-to-center spacing between the second and third solitons is reduced to just 18 waveguides, thus their interaction is strong now. By analyzing the trajectory of the second and third solitons, one can see that the soliton with label 3′ (2′) is the natural continuation of the second (third) soliton. However, by analyzing the peak amplitude and width of the input solitons (second, third) and the output ones (solitons with labels 2′, 3′), from Fig. 3(d) one can see that the soliton with label 2′ (3′) is more similar to the second (third) soliton, and thus in terms of soliton profiles the soliton with label 2′ (3′) is the natural continuation of the second (third) soliton. So, we have the difference between conclusions based on the soliton trajectories and those based on the soliton profiles. One of possible interpretations is that the soliton with label 3′ (2′) is the continuation of the second (third) soliton, and the profile difference between the soliton with label 3′ (2′) and the second (third) soliton is due to the energy exchange between interacting solitons when they are brought together close enough at the distance $z \simeq 390$. Another possible interpretation is that the second and third solitons just somehow *tunnel* through each other when they are brought closely enough, and after that each soliton just continues its path: the soliton with label 2′ (3′) is the continuation of the second (third) soliton. However, we would like to stress that the final interpretation of this peculiar behavior in Fig. 3(d) is still open to discussion.

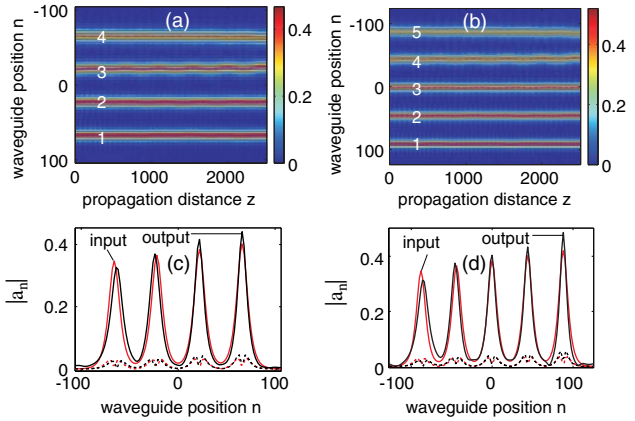

Fig. 4. (a), (b) Interaction of four and five Dirac solitons, respectively. (c) The input and output soliton profiles taken from (a) with the initial parameter $r = 1.1, 1.05, 1.0, 0.95$ from the first to fourth quasi-solitons. (d) The input and output soliton profiles taken from (b) with the initial parameter $r = 1.15, 1.1, 1.05, 1.0, 0.95$ from the first to fifth quasi-solitons. All quasi-solitons are initially in-phase, spacing between two adjacent quasi-solitons is 44 waveguides, the other parameters are the same as in Fig. 1.

In the rest of this paper we investigate the interaction of four and five Dirac quasi-solitons that are initially in-phase. The propagation of four and five Dirac quasi-solitons is demonstrated in Figs. 4(a) and 4(b), respectively. The input and output profiles of four and five Dirac quasi-solitons are shown in Figs. 4(c) and 4(d), respectively, where red (black) curves plot the input (output) profiles. In Figs. 4(a) and 4(c), each Dirac quasi-soliton (from the first to fourth one) is obtained by multiplying the exact Dirac soliton solution with the parameter $r = 1.1, 1.05, 1.0$, and 0.95, respectively. In Figs. 4(b) and 4(d), the parameter $r = 1.15, 1.1, 1.05, 1.0$, and 0.95 is used for the corresponding quasi-soliton (from the first to fifth one), respectively. One can see from Figs. 4(a) and 4(b) that these complex structures are quite robust. Even though at the input we use the Dirac quasi-solitons with different values of the parameter r, during propagation these Dirac quasi-solitons evolve toward the exact Dirac solitons. This is true not only for a single Dirac quasi-soliton, as shown in Fig. 1, but also for a complex of interacting Dirac quasi-solitons. Indeed, as shown in Figs. 4(c) and 4(d), Dirac quasi-solitons with parameter $r < 1$ [fourth quasi-soliton in Figs. 4(a) and 4(c) and fifth quasi-soliton in Figs. 4(b) and 4(d)] will evolve toward Dirac solitons with lower peak amplitudes and wider widths, which is in agreement with results shown in Fig. 1(d). Meanwhile, Dirac quasi-solitons with parameter $r > 1$ [first, second quasi-solitons in Figs. 4(a) and 4(c); and first, second, third quasi-solitons in Figs. 4(b) and 4(d)] will evolve toward Dirac solitons with higher peak amplitudes and narrower widths, which is also in agreement with results shown in Fig. 1(c). The robustness of these Dirac quasi-soliton complexes and the evolution of interacting Dirac quasi-solitons toward exact Dirac solitons once again confirm the stability of Dirac solitons.

4. CONCLUSION

In conclusion, we demonstrate numerically that discrete spatial solitons found in BWAs—optical analogs of relativistic

Dirac solitons in a nonlinear extension of the 1D Dirac equation describing the dynamics of a freely moving relativistic particle—are stable. Even though the initial beam can be different from the exact soliton, during propagation in BWAs the beam can gradually evolve toward the exact soliton. During propagation, it is also possible to form stable structures consisting of many interacting Dirac solitons from inputs made of many quasi-solitons that initially have slightly different peak amplitudes. Many interaction features of these solitons are similar to those of NLSE solitons: two in-phase solitons will attract each other and two out-of-phase solitons will repel each other, they can also exchange energy for intermediate values of phase difference between two solitons. However, the interaction behavior of two in-phase discrete spatial solitons in BWAs is quite different from that of two in-phase NLSE solitons at the later stage after the first collision. Unlike two NLSE in-phase interacting solitons where periodic pattern (including collision) is formed, the collision between two solitons in BWAs happens more and more frequently, and finally just one beam is formed. Our results suggest that BWAs can be used as a classical simulator to investigate the interaction between relativistic Dirac solitons, enabling to realize an experimentally accessible model system of quantum nonlinearities that have been so far a subject of speculation in the foundation of quantum field theories.

ACKNOWLEDGMENTS

This work is supported by the German Max Planck Society for the Advancement of Science (MPG) through the program for Max Planck Partner Groups. The authors would like to acknowledge F. Biancalana for useful suggestions.

REFERENCES

1. F. Lederer, G. I. Stegeman, D. N. Christodoulides, G. Assanto, M. Segev, and Y. Silberberg, "Discrete solitons in optics," Phys. Rep. **463**, 1–126 (2008).
2. T. Pertsch, P. Dannberg, W. Elflein, A. Bräuer, and F. Lederer, "Optical Bloch oscillations in temperature tuned waveguide arrays," Phys. Rev. Lett. **83**, 4752–4755 (1999).
3. R. Morandotti, U. Peschel, J. S. Aitchison, H. S. Eisenberg, and Y. Silberberg, "Experimental observation of linear and nonlinear optical Bloch oscillations," Phys. Rev. Lett. **83**, 4756–4759 (1999).
4. M. Ghulinyan, C. J. Oton, Z. Gaburro, L. Pavesi, C. Toninelli, and D. S. Wiersma, "Zener tunneling of light waves in an optical superlattice," Phys. Rev. Lett. **94**, 127401 (2005).
5. H. Trompeter, T. Pertsch, F. Lederer, D. Michaelis, U. Streppel, A. Bräuer, and U. Peschel, "Visual observation of Zener tunneling," Phys. Rev. Lett. **96**, 023901 (2006).
6. S. Longhi, M. Marangoni, M. Lobino, R. Ramponi, P. Laporta, E. Cianci, and V. Foglietti, "Observation of dynamic localization in periodically curved waveguide arrays," Phys. Rev. Lett. **96**, 243901 (2006).
7. Y. Lahini, A. Avidan, F. Pozzi, M. Sorel, R. Morandotti, D. N. Christodoulides, and Y. Silberberg, "Anderson localization and nonlinearity in one-dimensional disordered photonic lattices," Phys. Rev. Lett. **100**, 013906 (2008).
8. Tr. X. Tran and F. Biancalana, "Diffractive resonant radiation emitted by spatial solitons in waveguide arrays," Phys. Rev. Lett. **110**, 113903 (2013).
9. Tr. X. Tran and F. Biancalana, "Mimicking the nonlinear dynamics of optical fibers with waveguide arrays: towards a spatiotemporal supercontinuum generation," Opt. Express **21**, 17539–17546 (2013).
10. Tr. X. Tran, D. C. Duong, and F. Biancalana, "Supercontinuum generation in both frequency and wave number domains in nonlinear waveguide arrays," Phys. Rev. A **89**, 013826 (2014).
11. S. Longhi, "Klein tunneling in binary photonic superlattices," Phys. Rev. B **81**, 075102 (2010).
12. F. Dreisow, R. Keil, A. Tünnermann, S. Nolte, S. Longhi, and A. Szameit, "Klein tunneling of light in waveguide superlattices," Europhys. Lett. **97**, 10008 (2012).
13. S. Longhi, "Photonic analog of *Zitterbewegung* in binary waveguide arrays," Opt. Lett. **35**, 235–237 (2010).
14. F. Dreisow, M. Heinrich, R. Keil, A. Tünnermann, S. Nolte, S. Longhi, and A. Szameit, "Classical simulation of relativistic *Zitterbewegung* in photonic lattices," Phys. Rev. Lett. **105**, 143902 (2010).
15. S. Longhi, "Classical simulation of relativistic quantum mechanics in periodic optical structures," Appl. Phys. B **104**, 453–468 (2011).
16. J. M. Zeuner, N. K. Efremidis, R. Keil, F. Dreisow, D. N. Christodoulides, A. Tünnermann, S. Nolte, and A. Szameit, "Optical analogues for massless Dirac particles and conical diffraction in one dimension," Phys. Rev. Lett. **109**, 023602 (2012).
17. Tr. X. Tran, S. Longhi, and F. Biancalana, "Optical analogue of relativistic Dirac solitons in binary waveguide arrays," Ann. Phys. **340**, 179–187 (2014).
18. Y. Nogami, F. M. Toyama, and Z. Zhao, "Nonlinear Dirac soliton in an external field," J. Phys. A **28**, 1413–1424 (1995).
19. A. A. Sukhorukov and Y. S. Kivshar, "Discrete gap solitons in modulated waveguide arrays," Opt. Lett. **27**, 2112–2114 (2002).
20. A. A. Sukhorukov and Y. S. Kivshar, "Generation and stability of discrete gap solitons," Opt. Lett. **28**, 2345–2347 (2003).
21. M. Conforti, C. De Angelis, and T. R. Akylas, "Energy localization and transport in binary waveguide arrays," Phys. Rev. A **83**, 043822 (2011).
22. R. Morandotti, D. Mandelik, Y. Silberberg, J. S. Aitchison, M. Sorel, D. N. Christodoulides, A. A. Sukhorukov, and Y. S. Kivshar, "Observation of discrete gap solitons in binary waveguide arrays," Opt. Lett. **29**, 2890–2892 (2004).
23. W. Heisenberg, "Quantum theory of fields and elementary particles," Rev. Mod. Phys. **29**, 269–278 (1957).
24. D. C. Ionescu, R. Reinhardt, B. Muller, and W. Greiner, "Nonlinear extensions of the Dirac equation and their implications in QED," Phys. Rev. A **38**, 616–620 (1988).
25. A. Zecca, "Dirac equation in space-time with torsion," Int. J. Theor. Phys. **41**, 421–428 (2002).
26. M. J. Esteban and E. Séré, "An overview on linear and nonlinear Dirac equations," Discrete Contin. Dyn. Syst. **8**, 381–397 (2002).
27. I. Bialynicki-Birula and J. Mycielski, "Nonlinear wave mechanics," Ann. Phys. **100**, 62–93 (1976).
28. L. H. Haddad and L. D. Carr, "The nonlinear Dirac equation in Bose-Einstein condensates: foundation and symmetries," Physica D **238**, 1413–1421 (2009).
29. L. H. Haddad and L. D. Carr, "Relativistic linear stability equations for the nonlinear Dirac equation in Bose-Einstein condensates," Europhys. Lett. **94**, 56002 (2011).
30. N. Kemmer, "Zur theorie der neutron-proton wechselwirkung," Helv. Phys. Acta **10**, 47–67 (1937).
31. E. Fermi and C. N. Yang, "Are mesons elementary particles?" Phys. Rev. **76**, 1739–1743 (1949).
32. G. P. Agrawal, *Nonlinear Fiber Optics*, 5th ed. (Academic, 2013).
33. Y. S. Kivshar and G. P. Agrawal, *Optical Solitons: From Fiber to Photonic Crystals*, 5th ed. (Academic, 2003).
34. V. E. Zakharov and A. B. Shabat, "Exact theory of two-dimensional self-focusing and one-dimensional self-modulation of waves in nonlinear media," Sov. Phys. JETP **34**, 62–69 (1972).
35. N. N. Rosanov and Tr. X. Tran, "Interaction of dissipative Bragg solitons in active nonlinear fibers," Chaos **17**, 037114 (2007).